2012 Southern California Earthquake Center Annual Report
Temporal changes of earthquake rate and seismic velocity in southern California following the 2010 M7.2 El Mayor-Cucapah Earthquake

Zhigang Peng (PI)
School of Earth and Atmospheric Sciences
Georgia Institute of Technology, Atlanta, GA, 30338
March 15, 2013

Summary

We conducted a systematic detection of missing earthquakes in Southern California following the El Mayor-Cucapah mainshock [Meng et al., 2012, 2013b]. By running the detection algorithm in parallel GPU settings, we can achieve several hundred times faster speed than running the job in standard desktop CPUs. So far we have detected about 20 times more earthquakes than listed in the SCSN catalog. The obtained seismicity rate changes suggest a clear increase of seismic activity in many regions, including those in stress shadows. However, the seismicity rates correlate better with static stress changes a few months later. These results suggested that dynamic stress changes dominant in the short-term, while static stress changes play a more important role at later time.

1. Recent Results on Detecting Earthquakes in Southern California

Whether static or dynamic stress changes is the dominant mechanism for triggering earthquakes in the near field is currently unclear [Felzer and Brodsky, 2006; Richards-Dinger et al., 2010]. Earthquake triggering usually depend on seismicity rate changes from earthquake catalogs. However, such catalogs are often incomplete immediately after the mainshock, which may cause apparent seismicity rate changes unrelated to stress changes [e.g., Peng et al., 2007]. The 2010 Mw7.2 El Mayor-Cucapah earthquake occurred in northern Baja California, and generated significant stress perturbations and seismicity rate changes in southern California.

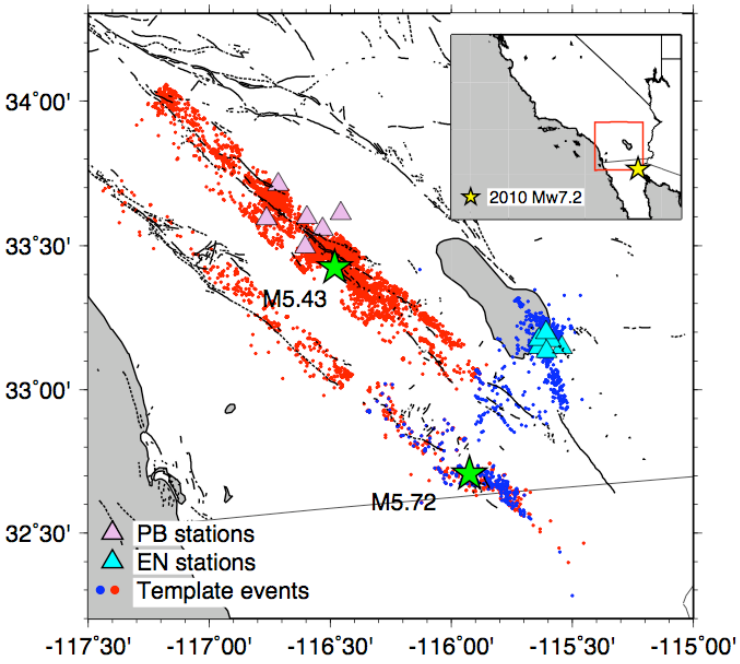

Figure 1. Map of southern California. The black traces are the major fault zones. The green stars are the two largest events in southern California following the mainshock. The blue and red template events use waveforms recorded by EN and PB stations, respectively. The inset map shows a large region around California and Mexico. The yellow star marks the epicenter of the mainshock.

In our last year's effort we focused primarily on the Salton Sea geothermal field (SSGF) and San Jacinto fault (SJF) mainly because of the significant stress changes following the mainshock, dense borehole seismic network coverage and abundant background seismicity (Figure 1). To get a more complete catalog, we apply a waveform-based matched filter technique to systematically detect possibly missing events near SSGF and SJF from 03/01/2010 until 08/01/2010. We run the detection codes on

multiple GPU clusters [Meng et al., 2012], significantly reducing the computation time. As a result, we detect ~20 times more events than listed in the Southern California Seismic Network (SCSN) catalog. Based on our detected events, the seismicity rate near SSGF and SJF both experienced significant increase immediately following the mainshock. However, the seismicity rate near SSGF, where static Coulomb Failure Stress (σ_{CFS}) decreased, dropped below the pre-mainshock level after ~50 days (Figure 2). On the other hand, the seismicity rate near SJF, where σ_{CFS} increased, remained high till the end of our detecting time window (Figure 3). Such pattern is consistent with dynamic stress changes being dominant in the short period, while sCFS changes may be more important in the longer term. Our next step is to apply the waveform detection technique to the entire southern California around the origin time of the El Mayor-Cucapah earthquake, and compare the seismicity rate changes with the peak dynamic and sCFS changes.

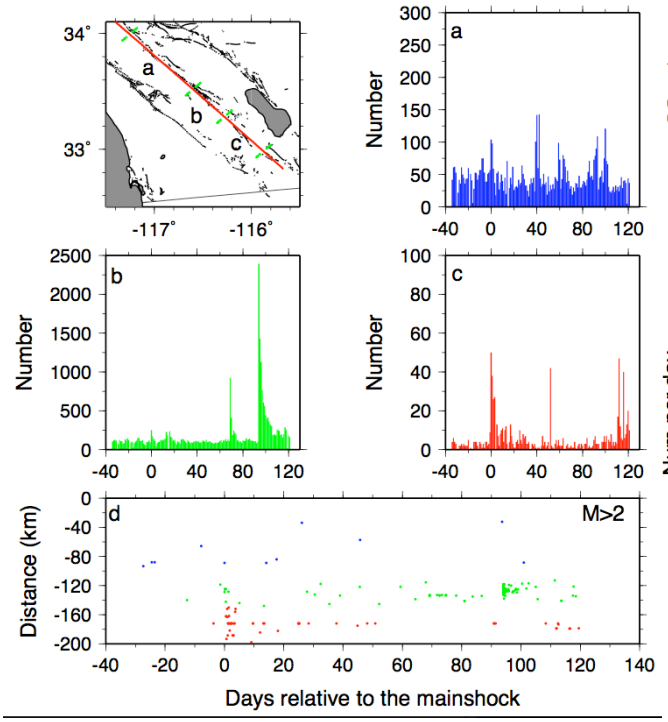

Figure 2. Seismicity rate changes along the San Jacinto Fault (SJF) zone. The map shows the three segments along the SJF; (a), (b) and (c) Number of events detected per day in segments a, b and c, respectively. (d) Spatial-temporal evolution of detected events with M>2 along the SJF. The dots are color coded by the segments they belong to.

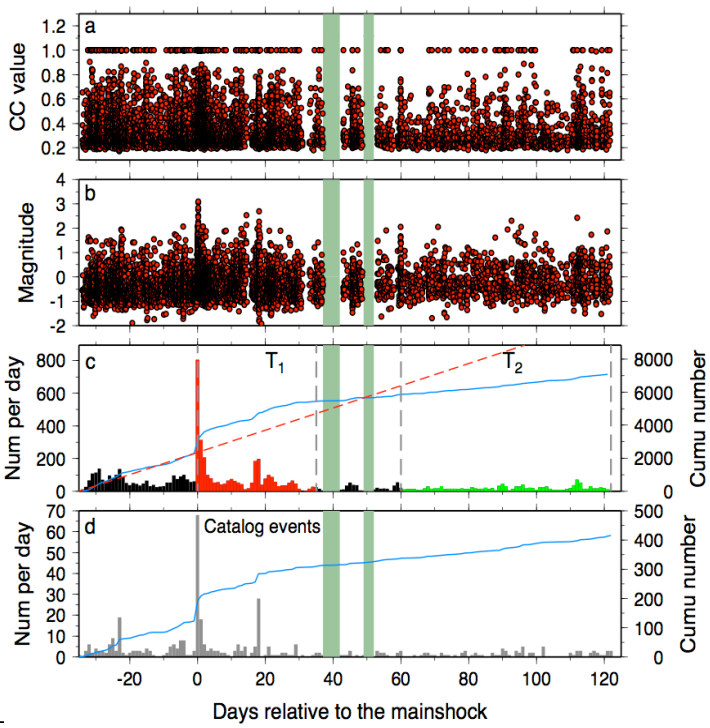

Figure 3. Seismicity rate changes near the Salton Sea geothermal field (SSGF). (a) and (b) CC and magnitude of detected events versus days relative to the mainshock, respectively. (c) Number of events detected per day. The blue curve shows the cumulative number of detected events. The red dashed line denotes the approximate pre-shock rate. (d) Number of events listed in the relocated catalog per day and the cumulative numbers.

Student Support and Involvement. This project provided a partial support for the GT graduate student Xiaofeng Meng, who is expected to finish his Ph.D. in May 2014. Xiaofeng has become an expert in this topic, as evident by several manuscripts published or submitted over the last two years. The results from this project will become a major component of his Ph.D. thesis. This project also provided a partial support for a summer intern Stephen Allman (Randolph College

undergraduate student) in summer 2012. Stephen worked together with Xiaofeng on detecting missing aftershocks following the 2011 Mw5.8 Virginia earthquake (Meng et al., 2013c). We have started working with Professor Kim Olsen's group at SDSU to use realistic rupture models for accurate estimations of both dynamic and static stress changes at many regions and compare with seismicity patterns [Meng et al., 2013]. We plan to release our detected catalogs and the computation code via peer-reviewed publications.

References (with publications/meeting abstracts supported by the grant marked in bold)

Felzer, K., and E. Brodsky (2006), Decay of aftershock density with distance indicates triggering by dynamic stress, *Nature,* 441, 735-738.

Peng, Z., H. Gonzalez-Huizar, K. Chao*, C. Aiken*, B. Moreno, and G. Armstrong* (2013), Tectonic tremor beneath Cuba triggered by the Mw8.8 Maule and Mw9.0 Tohoku-Oki earthquakes, *Bull. Seismol. Soc. Am.*, 103(1), 595-600, doi: 10.1785/0120120253.

Felzer, K., and E. Brodsky (2006), Decay of aftershock density with distance indicates triggering by dynamic stress, *Nature,* 441, 735-738.

Meng*, X., X. Yu, Z. Peng and B. Hong (2012), Detecting earthquakes around Salton Sea following the 2010 M_w7.2 El Mayor-Cucapah earthquake using GPU parallel computing, *Procedia Computer Science*, 9, 937-946.

Meng*, X., Z. Peng, and J. Hardebeck (2013a), Seismicity around Parkfield correlates with static shear stress changes following the 2003 Mw6.5 San Simeon earthquake, *J. Geophys. Res.*, submitted.

Meng, X. Z. Peng, K. Withers, K. Olsen, X. Yu and B. Hong (2013b), Systematic Search of Missing Earthquakes Near the Salton Sea Geothermal Field and San Jacinto Fault Around the 2010 Mw7.2 El Mayor-Cucapah Earthquake, Seismol. Res. Lett., 84(2), 391.

Meng, X., S. Allman, Z. Peng and T. Gilstrap (2013b), Hurricane Irene's Impacts on the Aftershock Sequence of the 2011 Mw5.8 Virginia Earthquake, Seismol. Res. Lett., Seismol. Res. Lett., 84(2), 391.

Richards-Dinger, K., R. Stein, and S. Toda (2010), Decay of aftershock density with distance does not indicate triggering by dynamic stress. *Nature*, *467*(7315), 583-586.